Research Article | Vol. 26, No. 6 | 19 Mar 2018 | OPTICS EXPRESS 6490
Optics EXPRESS

# 295-kW peak power picosecond pulses from a thulium-doped-fiber MOPA and the generation of watt-level >2.5-octave supercontinuum extending up to 5 μm

**SIJING LIANG,* LIN XU, QIANG. FU, YONGMIN JUNG, DAVID P. SHEPHERD, DAVID J. RICHARDSON, AND SHAIF-UL ALAM**

*Optoelectronics Research Centre, University of Southampton, SO17 1BJ, UK*
**sl13g14@soton.ac.uk*

**Abstract:** We report a gain-switched diode-seeded thulium doped fiber master oscillator power amplifier (MOPA) producing up to 295-kW picosecond pulses (35 ps) at a repetition rate of 1 MHz with a good beam quality ($M^2$ ~1.3). A narrow-band, grating-based filter was incorporated within the amplifier chain to restrict the accumulation of nonlinear spectral broadening and counter-pumping of a short length of large-mode-area (LMA) fiber was used in the final stage amplifier to further reduce nonlinear effects. Finally, we generated watt-level >2.5-octave supercontinuum spanning from 750 nm to 5000 nm by using the MOPA output to pump an indium fluoride fiber.



**OCIS codes**: (060.2320) Fiber optics amplifiers and oscillators; (140.3510) Lasers, fiber.

## References and links

1. S. Ishii, K. Mizutani, H. Fukuoka, T. Ishikawa, B. Philippe, H. Iwai, T. Aoki, T. Itabe, A. Sato, and K. Asai, "Coherent 2 microm differential absorption and wind lidar with conductively cooled laser and two-axis scanning device," Appl. Opt. **49**(10), 1809–1817 (2010).
2. I. Mingareev, F. Weirauch, A. Olowinsky, L. Shah, P. Kadwani, and M. Richardson, "Welding of polymers using a 2μm thulium fiber laser," Opt. Laser Technol. **44**(7), 2095–2099 (2012).
3. N. M. Fried and K. E. Murray, "High-power thulium fiber laser ablation of urinary tissues at 1.94 μm," J. Endourol. **19**(1), 25–31 (2005).
4. L. Xu, Q. Fu, S. Liang, D. P. Shepherd, D. J. Richardson, and S.-U. Alam, "Thulium-fiber-laser-pumped, high-peak-power, picosecond, mid-infrared orientation-patterned GaAs optical parametric generator and amplifier," Opt. Lett. **42**(19), 4036–4039 (2017).
5. A. M. Heidt, J. H. V. Price, C. Baskiotis, J. S. Feehan, Z. Li, S. U. Alam, and D. J. Richardson, "Mid-infrared ZBLAN fiber supercontinuum source using picosecond diode-pumping at 2 μm," Opt. Express **21**(20), 24281–24287 (2013).
6. D. J. Richardson, J. Nilsson, and W. A. Clarkson, "High power fiber lasers: current status and future perspectives [Invited]," J. Opt. Soc. Am. B **27**(11), B63–B92 (2010).
7. S. D. Jackson, "Towards high-power mid-infrared emission from a fiber laser," Nat. Photonics **6**(7), 423–431 (2012).
8. G. Stevens and A. Robertson, "Fibre laser component technology for 2-micron laser systems," Proc. SPIE **9135**, 91350N (2014).
9. X. Wang, X. Jin, P. Zhou, X. Wang, H. Xiao, and Z. Liu, "All-fiber high-average power nanosecond-pulsed master-oscillator power amplifier at 2 μm with mJ-level pulse energy," Appl. Opt. **55**(8), 1941–1945 (2016).
10. Y. Tang, X. Li, Z. Yan, X. Yu, Y. Zhang, and Q. Wang, "50-W 2-μm nanosecond all-fiber-based thulium-doped fiber amplifier," IEEE J. Sel. Top. Quantum Electron. **20**(5), 537–543 (2014).
11. L. Li, B. Zhang, K. Yin, L. Yang, and J. Hou, "1 mJ nanosecond all-fiber thulium-doped fiber laser at 2.05 μm," Opt. Express **23**(14), 18098–18105 (2015).
12. C. Gaida, M. Gebhardt, P. Kadwani, L. Leick, J. Broeng, L. Shah, and M. Richardson, "Amplification of nanosecond pulses to megawatt peak power levels in $Tm^{3+}$-doped photonic crystal fiber rod," Opt. Lett. **38**(5), 691–693 (2013).
13. D. Strickland and G. Mourou, "Compression of amplified chirped optical pulses," Opt. Commun. **55**(6), 447–449 (1985).

#314808 https://doi.org/10.1364/OE.26.006490
Journal © 2018 Received 1 Dec 2017; revised 17 Jan 2018; accepted 19 Jan 2018; published 5 Mar 2018

Optics EXPRESS

14. P. Wang, L. Yang, and J. Liu, "156 micro-J ultrafast Thulium-doped fiber laser," in *SPIE Photonics West* (2013), pp. 8601.
15. F. Stutzki, C. Gaida, M. Gebhardt, F. Jansen, C. Jauregui, J. Limpert, and A. Tünnermann, "Tm-based fiber-laser system with more than 200 MW peak power," Opt. Lett. **40**(1), 9–12 (2015).
16. A. M. Heidt, Z. Li, and D. J. Richardson, "High Power Diode-Seeded Fiber Amplifiers at 2 μm – From Architectures to Applications," IEEE J. Sel. Top. Quantum Electron. **20**(5), 525–536 (2014).
17. J. Liu, C. Liu, H. Shi, and P. Wang, "High-power linearly-polarized picosecond thulium-doped all-fiber master-oscillator power-amplifier," Opt. Express **24**(13), 15005–15011 (2016).
18. S. Guillemet, Y. Hernandez, D. Mortag, F. Haxsen, A. Wienke, D. Wandt, L. Leick, and W. Richter, "High energy sub-nanosecond thulium-doped all-fibre laser based on a rod-type photonic-crystal fibre amplifier," in *Advanced Solid State Lasers*, OSA Technical Digest (online) (Optical Society of America, 2015), paper ATh2A.27.
19. G. P. Agrawal, "Modulation Instability in Erbium-Doped Fiber Amplifiers," IEEE Photonics Technol. Lett. **4**(6), 562–564 (1992).
20. R. Phelan, J. O'Carroll, D. Byrne, C. Herbert, J. Somers, and B. Kelly, "$In_{0.75}Ga_{0.25}As$/InP Multiple Quantum-Well Discrete-Mode Laser Diode Emitting at 2 μm," IEEE Photonics Technol. Lett. **24**(8), 652–654 (2012).
21. G. P. Agrawal, *Nonlinear Fiber Optics* (Academic Press, 2013).
22. E. Desurvire, "Analysis of gain difference between forward- and backward-pumped erbium-doped fiber amplifiers in the saturation regime," IEEE Photonics Technol. Lett. **4**(7), 711–714 (1992).
23. J. M. Dudley and J. R. Taylor, *Supercontinuum generation in optical fibers* (Cambridge University, 2010).
24. K. Liu, J. Liu, H. Shi, F. Tan, and P. Wang, "High power mid-infrared supercontinuum generation in a single-mode ZBLAN fiber with up to 21.8 W average output power," Opt. Express **22**(20), 24384–24391 (2014).
25. G. Qin, X. Yan, C. Kito, M. Liao, C. Chaudhari, T. Suzuki, and Y. Ohishi, "Ultrabroadband supercontinuum generation from ultraviolet to 6.28 μm in a fluoride fiber," Appl. Phys. Lett. **95**(16), 161103 (2009).
26. J. C. Gauthier, V. Fortin, J. Y. Carrée, S. Poulain, M. Poulain, R. Vallée, and M. Bernier, "Mid-IR supercontinuum from 2.4 to 5.4 μm in a low-loss fluoroindate fiber," Opt. Lett. **41**(8), 1756–1759 (2016).
27. M. Michalska, J. Mikolajczyk, J. Wojtas, and J. Swiderski, "Mid-infrared, super-flat, supercontinuum generation covering the 2-5 μm spectral band using a fluoroindate fibre pumped with picosecond pulses," Sci. Rep. **6**(1), 39138 (2016).

## 1. Introduction

Thulium doped fiber lasers (TDFLs) have experienced rapid development in the past few years, driven by a diverse range of applications including gas sensing, laser processing of both polymers and biological tissues, and nonlinear frequency conversion [1–5]. In contrast to ytterbium doped fiber lasers (YDFLs) which have a relatively narrow operating bandwidth at 1 μm, TDFLs have an exceptionally wideband emission spectrum covering 1.65–2.1 μm, which offers flexible wavelength tuning for various applications [6]. Moreover, the longer emission wavelength allows a larger core area while maintaining fundamental-mode operation. The larger mode areas increase the power-scaling potential of high peak power TDFLs by a factor of 4 or so as compared to YDFLs [7].

The recent rapid progress in fiber-component technology at 2 microns is accelerating the development of continuous wave (CW) and pulsed thulium doped fiber lasers [8]. Numerous publications have reported nanosecond thulium doped fiber lasers with high average output power, which are desirable for applications such as materials processing [9–11]. For example, X. Wang *et al*. recently presented a nanosecond-pulsed thulium-doped LMA-fiber MOPA system with an average output power scalable from 150 W to 238 W [9]. Additionally, nanosecond pulses with up to 4-MW peak power were successfully demonstrated from a rod-type thulium-doped photonic-crystal-fiber amplifier with a core diameter of 80 μm [12]. Chirped pulse amplification (CPA) provides an easier route to scale the peak power of femtosecond pulses to the MW level, however dispersion management and pulse compression add to the system complexity [13]. P. Wang *et al*. and F. Stutzki *et al*. reported femtosecond pulses with a peak power in excess of 200 MW from a CPA system based on a LMA thulium doped fiber with 25-μm core diameter and a thulium-doped large-pitch rod fiber with a mode field diameter of 65 μm, respectively [14,15]. Alternatively, high-power picosecond lasers can be a good option for many nonlinear frequency conversion applications due to the simpler system architectures compared to femtosecond CPA systems and much shorter pulse duration in comparison to nanosecond lasers [16]. An all-fiber linearly-polarized picosecond thulium doped fiber MOPA system was demonstrated by J. Liu *et al*. with the current highest average

Optics EXPRESS

power of 240 W, which is comparable to the average power of many nanosecond thulium doped fiber lasers [17]. A. M. Heidt *et al.* reported a thulium-doped LMA-fiber-based MOPA system which yielded 40-ps pulses with 130-kW peak power while S. Guillemet *et al.* achieved 520-ps pulses with a peak power of up to 230 kW from a thulium doped photonic crystal rod fiber with an 80-μm core diameter [16,18]. At the 2-μm waveband, nonlinear effects such as four-wave mixing (FWM) and modulation instability (MI) are the major constraints of the maximum accessible peak power because of the transfer of pulse energy to out-of-band noise at high peak powers. Furthermore, an input signal that incorporates additional spectral sidebands may act as a seed for these adverse effects and lower the nonlinear threshold even further [19]. Hence, careful management of fiber nonlinearity and signal purity are essential to accomplish further power scaling from thulium-doped fiber MOPA systems.

Here we report the generation of picosecond pulses with record-breaking peak power of 295 kW from a diode-seeded fiber MOPA system based on a short piece of backward-pumped LMA fiber in conjunction with in-line spectral filtering. We also achieved 2.7-octave-spanning, flat-spectral-profile, mid-infrared supercontinuum generation by launching the output of the MOPA into an indium fluoride fiber.

## 2. Experimental setup

Figure 1 shows a schematic of the MOPA system. A seed diode at 1953 nm (Eblana Photonics) was gain-switched using 420-ps electrical pulses at 1-MHz repetition rate. The seed pulses were first amplified by a core-pumped thulium doped fiber amplifier (TDFA) using a 16-m-long thulium doped fiber (OFS TmDF200) pumped by an in-house built Er/Yb co-doped fiber laser at 1565 nm. Isolators were used at both the input and output of the amplifier to prevent signal feedback into the seed laser and amplified spontaneous emission (ASE) cross-coupling from the follow-on amplification stage, respectively. ASE generated in the first preamplifier stage was eliminated by a synchronized electro-optic modulator (EOM) (Photline MX2000-LN-01), which functioned as a time gate to pass the optical pulses but reject the accumulated ASE. A polarization controller and a fast-axis-blocked polarization-maintaining (PM) isolator were used to ensure linearly polarized light with maximum signal power coupled into the EOM. The second preamplifier was also a core-pumped TDFA incorporating a 1.2-m length of in-house fabricated thulium doped fiber with a core diameter of 8.5 μm and ~95 dB/m absorption at 1565 nm. The short device length and larger core size effectively suppressed the nonlinearities in the second stage amplifier. A grating-based filter comprising a pair of circulators and fiber Bragg gratings (FBGs) at 1953 nm acted as a narrow passband filter and removed unwanted spectral components as well as the ASE in the second stage preamplifier. The bandwidths of the first and the second gratings were 0.8 nm and 0.5 nm respectively. The high insertion loss of the grating filters necessitated a third preamplifier to boost the signal power to seed the final stage amplifier. The third stage preamplifier was built with a 2.5-m-long in-house fabricated double-clad thulium doped fiber and was pumped by a multimode laser diode at 790 nm with pump power of up to 9 W. The fiber had a core/cladding diameter of 11/127 μm and a cladding absorption of ~6 dB/m at 790 nm. The output of the third preamplifier was launched through a mode field adaptor into the final amplifier, which employed a LMA thulium doped fiber with a core/cladding diameter of 25/250 μm and an NA of 0.09/0.46 (Nufern). The mode field adaptor helped match the fundamental mode of the two dissimilar fibers and reduced the splice loss to ~1 dB. The final stage amplifier was free-space counter-pumped by two 790-nm multimode pump laser diodes, which were combined by a (2 + 1) × 1 pump and signal combiner. These pump diodes can deliver maximum pump power of up to 60 W. Only a 1.3-m length of LMA thulium doped fiber was used as the final-stage gain medium, absorbing more than 92% of the launched pump power. The output end had an angle-polished core-less end cap, which reduced the optical intensity at the glass-air interface and prevented optical damage to the end facet.

Optics EXPRESS

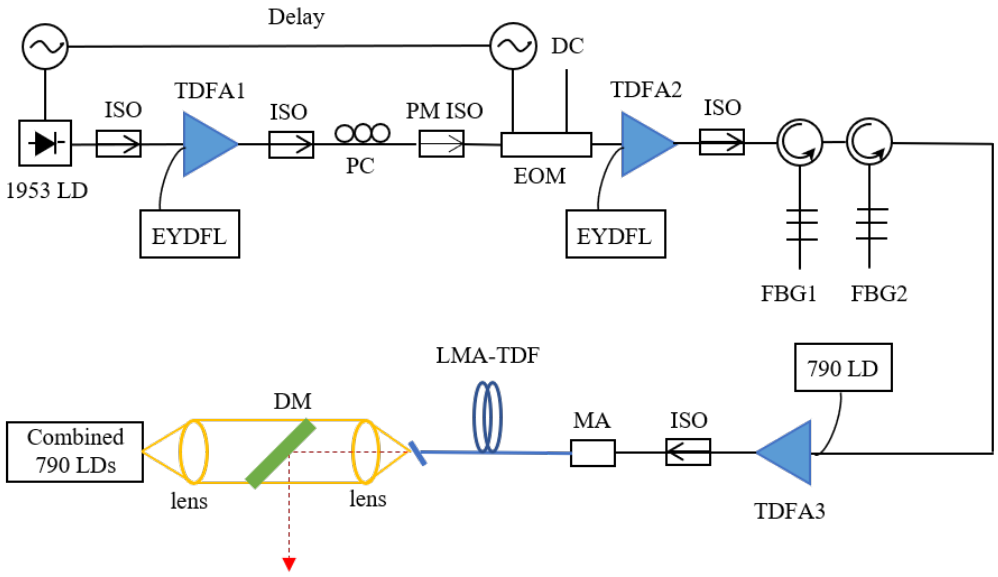


Fig. 1. Schematic of the MOPA system. 1953 LD: laser diode at 1953nm; ISO: isolator; EYDFL: Erbium/Ytterbium co-doped fiber laser; PC: polarization controller; PM ISO: polarization maintaining isolator; DC: direct current; EOM: electro-optic modulator; FBG: fiber Bragg grating; 790 LD: Laser diode at 790nm; MA: mode adaptor; LMA-TDF: large-mode-area thulium doped fiber; DM: dichroic mirror.

## 3. Results and discussions

### *3.1 Generation of high-energy picosecond pulses*

The seed laser was a low power InGaAs/InP ridge waveguide Fabry-Perot (FP) diode with slot features etched into the waveguide. The etched features enabled discrete mode operation by strengthening one FP mode and suppressing the others [20]. As depicted by the blue line in Fig. 2(a), the seed diode operating in the CW mode emitted a single longitudinal mode at 1952.8 nm with a narrow 3-dB spectral bandwidth of less than 0.1 nm, an excellent side mode suppression ratio (SMSR) of up to 45 dB, and a mode spacing of 1.5 nm. In contrast, gain-switching led to a broadening of the 3-dB spectral bandwidth to 0.9 nm (red line) with two longitudinal modes emitted at the same time. The relative intensity ratio of these two adjacent modes was ~3 dB. The average power of the gain-switched pulse train was ~1 μW. A fast photodetector (EOT, ET-5000F) was used to measure the pulse width, which was found to be ~100 ps as shown in Fig. 3(a). The first preamplifier (TDFA 1) provided high signal gain (~40 dB) but generated a lot of ASE in between the pulses because of the relatively low duty cycle (<0.01%), as indicated by the poor optical signal-to-noise ratio (OSNR) of 6 dB (green line). The OSNR improved to ~25 dB (cyan line) by temporally gating the pulses to remove the ASE between pulses. The EOM and associated polarization-sensitive components induced 9.7-dB of insertion loss and consequently the average output power after the EOM was only 1.2 mW.

Optics EXPRESS

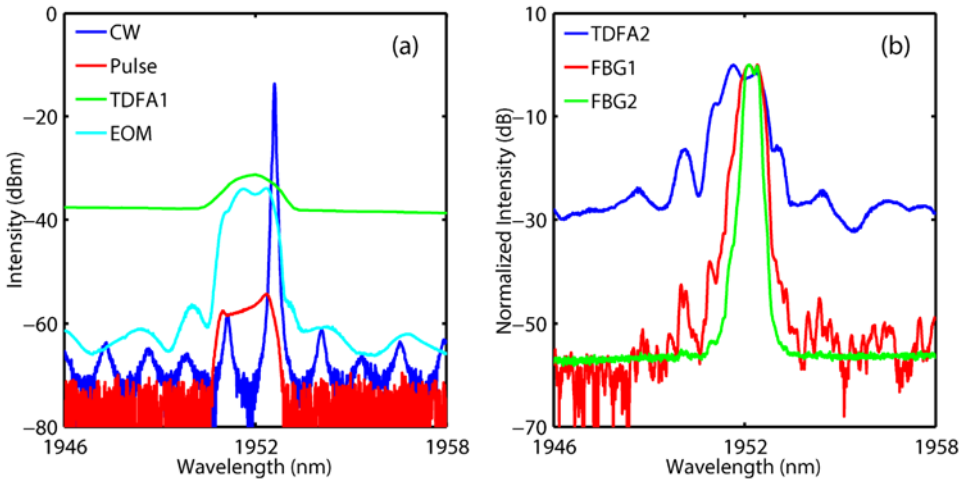


Fig. 2. (a) Spectra of the seed diode in CW and pulsed operation, as well as the outputs of the TDFA1 and EOM (0.05 nm resolution); (b) Spectra at the outputs of TDFA2, FBG1 and FBG2 (0.05 nm resolution).

Figure 2(b) shows the spectra at the output of the second preamplifier (TDFA 2) and after the grating filters used to clean up the output spectrum. The second preamplifier amplified the signal to 48 mW without significant nonlinear distortion. However, the dual longitudinal modes from the gain-switched diode served as a seed for FWM, producing multiple sidebands and impairing the signal spectrum. In order to reduce the signal impairment due to nonlinearities in the cascaded amplification stages, only the strongest longitudinal mode was picked out by using narrow-band gratings to seed the subsequent amplifiers. The grating filters removed the unwanted spectral components and achieved a greatly improved SMSR of up to 55 dB at the output (green line). The relatively high insertion loss (~9.8 dB) introduced by the grating filters necessitated the use of a third preamplifier stage (TDFA 3) to compensate the loss and increase the signal power into the final stage amplifier to 57 mW. The pulses after the second and the third preamplifier stages were measured with an autocorrelator and the results are shown in Fig. 3(b). The measured Gaussian-shape autocorrelation (AC) traces had a full width at half maximum (FWHM) of 74 ps and 49 ps, corresponding to a pulse duration of 52 ps and 35 ps respectively. The pulses were continuously compressed along the amplifier chain as a result of the interplay between dispersion and self phase modulation (SPM), a behavior that is well documented in the literature [16].

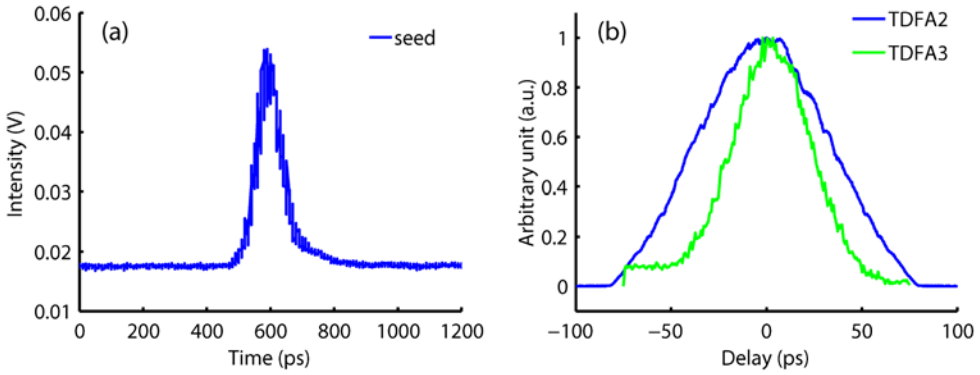


Fig. 3. (a) Temporal profile of the seed pulse measured by a fast photodetector; (b) Autocorrelation traces measured after the second and the third preamplifier.

Optics EXPRESS

The final amplifier scaled up the signal power to 10.34 W at a slope efficiency of 29.5% and with no power roll-off observed after continuous operation for many hours (Fig. 4). A maximum signal gain of 22.5 dB was obtained from this amplification stage. Figure 4(b) plots the AC trace measured at the output. The AC trace had a FWHM of 49 ps corresponding to a FWHM Gaussian pulse width of 35 ps. The pulse width remained constant before and after the final amplifier at different output powers. The estimated maximum pulse energy is 10.34 µJ corresponding to a pulse peak power of 295 kW. Figure 5 presents the output spectral evolution with increasing output signal power. The signal maintained an extraordinary out-of-band OSNR of at least 40 dB. The onset of MI only became noticeable at the highest output power with two symmetrical MI sideband peaks located at ~1920 nm and ~1980 nm respectively, prohibiting further power scaling of the current system. The observation of MI sidebands is common in the 2-µm waveband due to the inherent anomalous dispersion of silica-based fibers. MI can be interpreted as a four-wave-mixing process that is phased matched by SPM. Therefore, SPM can initiate and facilitate the growth of MI when the frequency components generated by SPM fall within the MI gain spectrum [21]. However, the effective nonlinear length of our final amplifier was minimized by counter-pumping an optimum length of LMA fiber and operating the amplifier in the high-gain regime, thereby minimizing nonlinear effects and enabling high peak power operation [22]. The 10-dB spectral bandwidth broadened from 0.6 nm at 1.024 W to 1.7 nm at 10.34 W, as shown in Fig. 5(b). The MOPA output has a near-diffraction-limited beam quality and this only degraded slightly from 1.2 at 4.5 W of average power to 1.3 at the maximum output power of 10.34 W.

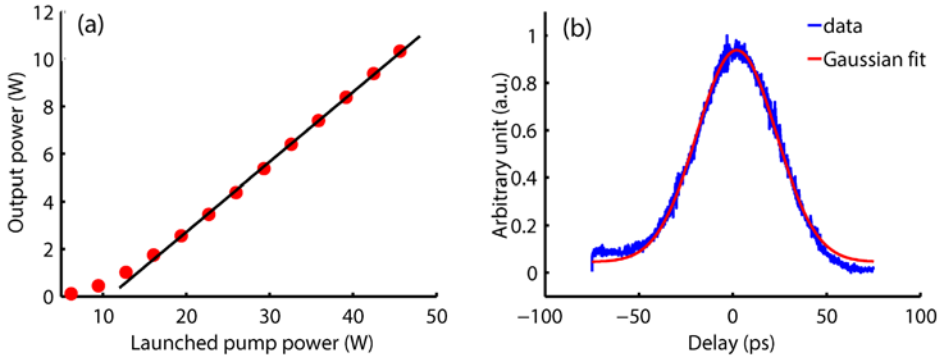


Fig. 4. (a) Power scaling of the final stage amplifier; (b) Autocorrelation trace measured at 4.5 W average output power and the corresponding Gaussian fit.

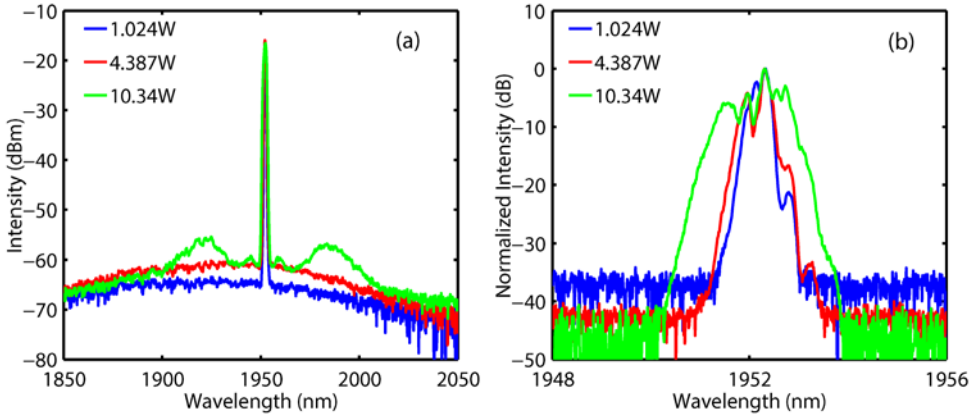


Fig. 5. (a) Broadband (1.0 nm resolution) and (b) high resolution (0.05 nm resolution) spectra of the MOPA system at 1.024 W, 4.387 W and 10.34 W average output powers.

Optics EXPRESS

### 3.2 Mid-IR supercontinuum generation

Supercontinuum generation in fluoride fibers has recently been widely studied because fluoride fibers have a wide transmission window from the visible to the mid infrared with a zero dispersion wavelength located between 1.5 and 1.8 μm, which can be accessed by high-power fiber lasers [23]. To date, supercontinuum generation based on fluorozirconate (ZBLAN) fibers has achieved impressive results, such as a broad output spectrum extending up to 4 μm and a watt-level average output power [5, 24]. Supercontinuum generation with average output power of up to 21.8 W from 1.9 to beyond 3.8 μm was obtained from a 10-m-long ZBLAN fiber pumped by a high-power thulium-doped fiber MOPA [24]. A broad output spectrum extending up to 4 μm with superb flatness (1.5 dB) from 2450 nm to 3750 nm was implemented by picosecond pumping a 7-m-long ZBLAN fiber at 2 μm [5]. The long wavelength edge of the supercontinuum can be driven up to 6.28 μm in extreme conditions such as using a centimeter-long ZBLAN fiber pumped by femtosecond pulses, but the output power was relatively low (<20 mW) and the flatness was barely satisfying [25]. For longer wavelength operation, fluoroindate fibers provide better alternative as compared to the ZBLAN fibers since they possess improved transparency between 4 and 5.5 μm, where strong absorption bands of carbon oxides are located. J. C. Gauthier *et al*. and M. Michalska *et al*. have successfully demonstrated supercontinuum generation beyond 5 μm in indium fluoride fibers, but their reported output powers were no more than 20 mW [26, 27]. The performance of supercontinuum generation in fluoroindate fibers has therefore been substantially behind that of ZBLAN-fiber-based supercontinuum sources.

Here, we launched the high peak power pulses from the MOPA into an indium fluoride fiber to investigate the possibility of high power supercontinuum generation extending out to 5 μm and beyond. The employed indium fluoride fiber (Thorlabs, S/N: A40038388) has a core/cladding diameter of 9/125 μm, core NA of 0.26, and a single-mode cutoff wavelength of 3.2 μm. The fiber has a transparency range covering 310 nm to 5.5 μm with an attenuation of less than 0.5 dB/m for 1.7–4.7 μm (Fig. 6). However, the fiber attenuation grows rapidly beyond 5 μm, reaching up to ~3 dB/m at 5.5 μm. The typical zero dispersion wavelength is around 1.7 μm, with a flat profile spanning from 2.5 μm to 4.5 μm, as shown in Fig. 6(b). The output of the MOPA was free-space coupled into a 10-m length of small-core indium fluoride fiber using an uncoated aspheric lens (f = 6.24 mm). Both fiber ends were flat cleaved and a polarization insensitive isolator (loss = ~0.8 dB) was placed before the coupling lens to protect the MOPA system from any unwanted back reflections. The coupling efficiency was measured to be ~55%.

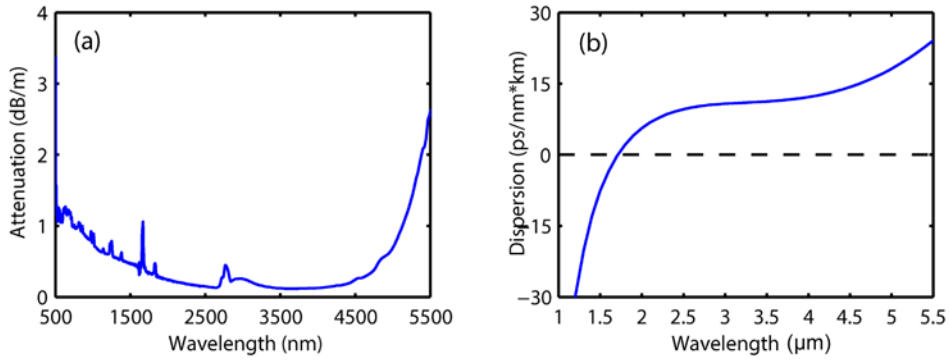


Fig. 6. (a) Attenuation of fluoroindate fibers; (b) dispersion profile of fluoroindate fibers (data provided by Thorlabs).

Figure 7 depicts the full-span spectra of the supercontinuum source with different incident peak powers. The output spectra were measured by an Ando AQ6317 optical spectrum analyzer (OSA) (700–1600 nm), a Yokogawa A6375 OSA (1600–2400 nm) and a Bentham

Optics EXPRESS

TMc300V monochromator with a liquid-nitrogen-cooled PbS detector for wavelengths above 2400 nm. The spectral resolutions of the OSAs and the monochromator were set to 2 nm and 10 nm respectively. Note that the OSAs and the monochromator have different noise floors. The relative power levels between instruments were calibrated with at least 100-nm spectral overlap during data acquisition. As the coupled peak power increased from 18.9 kW to 94.3 kW, the supercontinuum broadened from 3690 nm to 5000 nm at the long wavelength edge. Further increasing the injected pulse energy did not improve the supercontinuum bandwidth, while the onset of fiber facet damage was observed at a coupled peak power of 100 kW. A similar damage threshold (~128 kW) was previously reported in the literature [27]. Fiber attenuation beyond 5 μm and below 750 nm is believed to be the main constraint on further spectral broadening. The spectra show a residual pump peak at 1953 nm that is about 15 dB above the generated supercontinuum but carries only a small fraction (~8%) of the total output power. Figure 8 plots the total power and the power generated for two interesting wavelength range as a function of coupled pulse energy. Spectral integration is used to estimate the power for different interesting wavebands. At the maximum pump power, a total average output power of 1.76 W was achieved with 0.56 W for wavelengths above 2900 nm and 0.33 W for wavelengths above 3500 nm. The conversion efficiencies defined as the ratio of power in the desired waveband to the total power were 32% ($\lambda$ > 2900 nm) and 19% ($\lambda$ > 3500 nm) respectively. The supercontinuum has a 3-dB spectral flatness over an 1870-nm span from 2500 nm to 4370 nm. The spectral dip at ~4200 nm was caused by carbon dioxide absorption inside the monochromator.

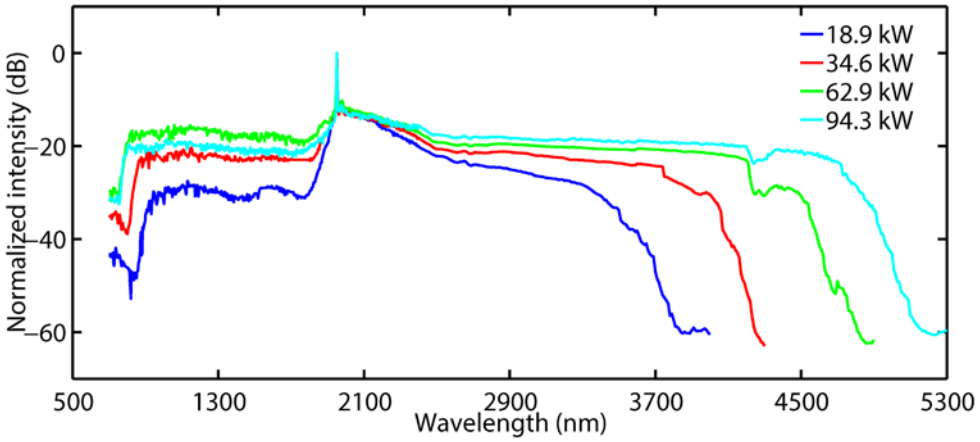


Fig. 7. Output supercontinuum spectra generated with different coupled pulse peak power.

Optics EXPRESS

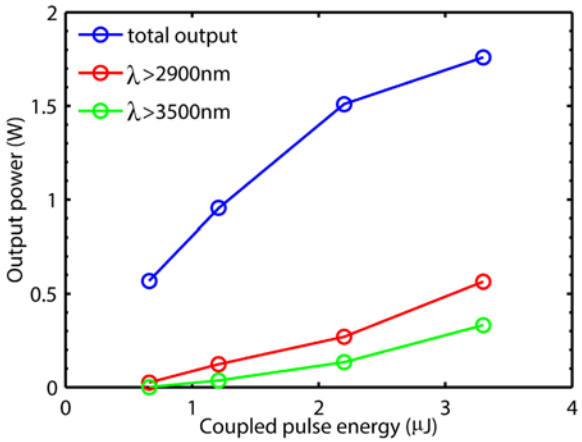


Fig. 8. Output power as a function of coupled pulse energy.

## 4. Conclusion

We have demonstrated the generation of high-peak-power picosecond pulses from a thulium doped fiber MOPA system seeded by a gain-switched laser diode. A maximum pulse energy of 10.34 μJ was obtained corresponding to a pulse peak power of 295 kW. The combination of spectral filtering and short device lengths enabled an increase in the nonlinear threshold of the whole system to achieve this record-breaking pulse peak power from a flexible thulium doped fiber MOPA with a very good beam quality. By pumping an indium fluoride fiber, we demonstrated >2.5-octave supercontinuum generation extending up to 5 μm with high average output powers and excellent spectral flatness.

## Funding

EPSRC AirGuide Photonics Programme Grant (Grant EP/P030181/1)

## Acknowledgment

The authors acknowledge Dr. Peter Shardlow from ORC for providing the in-house fabricated thulium doped fibers.